International Journal of Advances in Engineering and Management (IJAEM)
Volume 7, Issue 4 April. 2025, pp: 1133-1139 www.ijaem.net ISSN: 2395-5252

Global Navigation Satellite (GNSS) Tropospheric Delay Estimation in Offa, Kwara State, Nigeria

Babatomiwa Victor Olayode
Department of Physics, University of Ilorin, Ilorin, Nigeria
Corresponding Author

Date of Submission: 17-04-2025 Date of Acceptance: 30-04-2025

ABSTRACT: This Hydrostatic delay is caused by the dry component in the atmosphere, while wet delay is caused exclusively by highly varying water vapor in the atmosphere. The hydrostatic delay makes up approximately 90% of the total tropospheric delay and depends entirely on the atmospheric weather characteristics in the troposphere. The hydrostatic delay in the zenith direction is characteristically about 2.30m. It is modelled using measurements of surface temperature and pressure. However, the wet delay depends on water vapor pressure, which is highly variable in space and time and cannot be modelled precisely with surface measurements.

Most global tropospheric delay models used vary from one latitudinal location to another and usually return it in the zenith direction which is then mapped to the slant. This study estimates the tropospheric delay for Offa using monthly mean tropospheric data for the years 2014 to 2024 obtained from the Nigerian Meteorological Agency (NIMET). Three tropospheric models, namely; the Saastamoinen model (driven by tropospheric data) called SAAS MODE 1, the Saastamoinen model (driven by default values) called SAAS MODE2 and UNB3M models were used, and results were compared. Here the obtained zenith delay is mapped from vertical to slant using the Chao, Niell, and TANE mapping function at an elevation angle of 2° to 90°. The results obtained show that there is a seasonal trend in SAAS MODE1 whereas it is not observed in SAAS MODE 2 and UNB3M. Two peaks are observed generally in the value of zenith tropospheric delay for SAAS MODE 1 for all the years, one in March and the other one in November with a kind of minimum in August. In the exceptional, especially years 2019 and 2020 where three peaks are observed in the values of zenith tropospheric delay for SAASMODE1, one in March and the others in February and October with a kind of minimum in August. Generally, there is a drop from the peak point in March to July there about and later rise around August the minimum point.

To compare the output of three mapping functions (Chao, Niell, and TANE) at elevations of 2° to 90°, SAAS MODE 1 and SAAS MODE 2 were used for year 2024 data. It is observed that the three mapping functions returned almost the same values from elevation 90° to about 10°. Major discrepancies are observed at an elevation of 5° and below in which the TANE value deviated completely from the other two models. This gives Chao and Niell a good edge over TANE.As far as the deviations are concerned, the TANE value is higher than the other two models by about30 m at the elevation angle of 2°.

From the results obtained, the Saastamoinen model (driven by tropospheric data) is more realistic being varies with season most especially the wet component.

KEYWORDS: GNSS, GPS, Troposphere, Delay, Estimation.

I. INTRODUCTION

One of the fundamental issues in GPS positioning is the ability to mitigate all source errors such as atmospheric delay errors e.g., tropospheric delay error and ionospheric delay error. The effect of the troposphere on GNSS signals appears as a delay in the signal traveling from the satellite to the receiver. This delay depends on the temperature, pressure, humidity, and the receiver satellite outlet, i.e., elevation. When radio signals propagate through the atmosphere, they will experience bending because the refractive index of the atmosphere varies with height and causes an excess path length.

Delay caused by the neutral atmosphere (troposphere, tropopause, stratosphere, and part of the mesosphere) is non-dispersive, or completely independent of the signal frequency

International Journal of Advances in Engineering and Management (IJAEM)
Volume 7, Issue 4 April. 2025, pp: 1133-1139 www.ijaem.net ISSN: 2395-5252

(for GPS frequencies). Tropospheric delay is measured in meters, and a typical zenith tropospheric delay would be 2.50 m, meaning that the troposphere causes a GPS range observation to have an apparent additional 2.50 m distance between the ground-based receiver and a satellite at the zenith [1].

Tropospheric delay comprises two components: hydrostatic and wet [2]. Hydrostatic delay is caused by the dry component in the atmosphere, while wet delay is caused exclusively by highly varying water vapor in the atmosphere. The hydrostatic delay makes up approximately 90% of the total tropospheric delay and depends entirely on the atmospheric weather characteristics in the troposphere. The hydrostatic delay in the zenith direction is characteristically about 2.30m [3] [4]. It can be modeled using measurements of surface temperature and pressure. However, the wet delay is contingent on water vapor pressure, which is extremely variable in space and time and cannot be modeled precisely with surface measurements [5].

More reliable and realistic tropospheric delays can be estimated from a model driven by tropospheric data from NIMET if the satellites and ground-based antenna positions are known. The obtained zenith delays can thus be mapped from vertical to slant using one of the available theoretical mapping functions such as [6][7][8] for station-satellite pairs.

II. RESEARCH METHODOLOGY

Tropospheric Delay Estimation

Acquisition of Data

The tropospheric data used for this study is obtained from the Nigerian Meteorological Agency (NIMET). The obtained data are monthly mean values of Offa (with coordinate; Latitude 8.9^0N, Longitude 4.43^0E, and Height 314m) for the years 2014 to 2024. They are as follows: Minimum temperature and Maximum temperature.
The following parameters were derived from the measured values, the related equations are given below;
Mean temperature.

$$T = \frac{(\max temp + \min temp)}{2} + 273 \quad (1)$$

Surface partial pressure of water vapor

$$ew = \frac{P}{760} \times e^{\left(20.386 - \frac{5132}{T}\right)} \quad (2)$$

Where,
ew is the surface partial pressure of water vapor in mbar
P =1013.25(the surface atmospheric pressure in hpa)
T is the temperature in kelvin
h = 0.148353(latitude of Offa in rad)
θ = 0.314 (Altitude of Offa in km)

The Models used for this study are; the Saastamoinen model driven with the tropospheric parameter (SAAS MODE 1), the Saastamoinen model driven with the default values (SAAS MODE 2), and the UNB3M Model.

Method of Analysis

In this study, SAASMODE1 is used for the estimation of tropospheric delay with tropospheric data as the input parameter compared with SAAS MODE 2 with default parameter as the input and UNB3M models. MATLAB R2024a software is used for the computation and analyses;

Zenith delays are converted to slant delay using equation (3).

$$SND = m(\varepsilon) \times ZND \quad (3)$$

Different mapping functions are being used for the conversion in equation (4).

$$SND(\varepsilon) = m_h(\varepsilon).\, ZHD + m_w(\varepsilon).\, ZWD \quad (4)$$

Where,
SND: slant neutral delay
m(ε): mapping function
$m_h(\varepsilon)$ hydrostatic mapping component
$m_w(\varepsilon)$ wet mapping component
ZND: zenith neutral delay
ZHD: zenith hydrostatic delay
ZWD: zenith wet delay

In this study, the zenith hydrostatic delay is estimated using the Saastamoinen model, while the wet delay is derived from precise measurements of surface atmospheric pressure using the equations (1) and (2). Zenith delays are converted into slant delay

International Journal of Advances in Engineering and Management (IJAEM)
Volume 7, Issue 4 April. 2025, pp: 1133-1139 www.ijaem.net ISSN: 2395-5252

satan elevation angle of 2° to 90°. These elevation angles are chosen to test the performance of the three-mapping function Chao, Niell, and TANE used in this study, to model the elevation dependence of the propagation delay.

III. RESULTS AND DISCUSSION

Zenith Delay

Figure1 shows the monthly plot of zenith tropospheric delay for the year 2014. It is observed that there is a seasonal trend in SAAS MODE1 whereas is not observed in SAAS MODE 2 and UNB3M. Two peaks are observed in the value of zenith tropospheric delay for SAAS MODE 1, one in March and the other one in November with a kind of minimum in August. There is and later a rise around September, a drop around May to July and later rises around August.

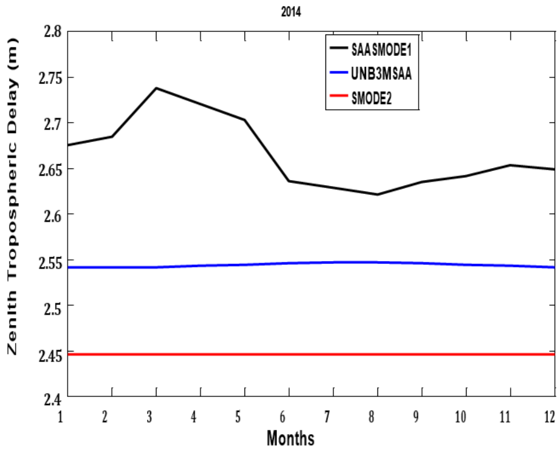

Figure1: Monthly plot of Zenith tropospheric delay for the year 2014

Figure 2 shows the monthly plot of Zenith tropospheric delay for the year 2017. It is observed that there is a seasonal trend in SAAS MODE1 whereas is not observed in SAASMODE2 and UNB3M.Three peaks are observed in the value of zenith tropospheric delay for SAAS MODE 1, one in March and the others in October and November with a kind of minimum in July till September, there was a drop around April to June.

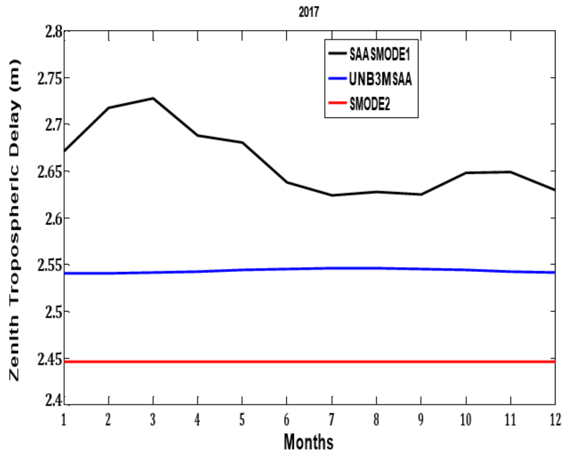

Figure 2: Monthly plot of Zenith tropospheric delay for the year 2017

Figure 3 shows the monthly plot of zenith tropospheric delay for the year 2021. It is observed that there are seasonal trends in SAAS MODE1 whereas is not observed in SAAS MODE 2 and UNB3M. Two peaks are observed in the value of zenith tropospheric delay for SAAS MODE 1, one is in March, and the other one is in November with a kind of minimum in August, there is a drop around April to July and a later rise around August.

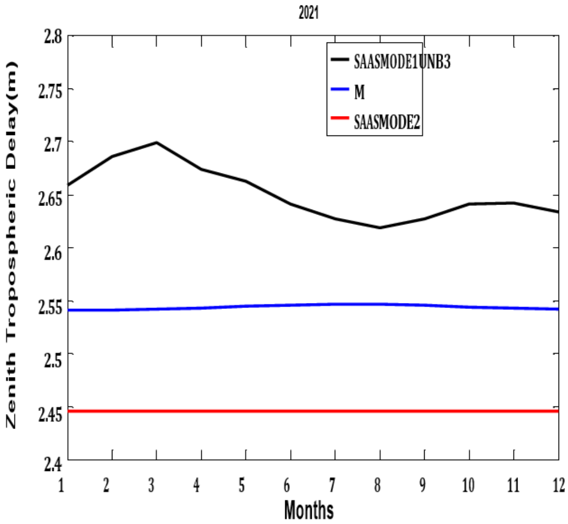

Figure 3: Monthly plot of Zenith tropospheric delay for the year 2021

International Journal of Advances in Engineering and Management (IJAEM)
Volume 7, Issue 4 April. 2025, pp: 1133-1139 www.ijaem.net ISSN: 2395-5252

Figure 4 shows the monthly plot of Zenith tropospheric delay for the year 2024. It is observed that there are seasonal trends in SAAS MODE1 whereas is not observed in SAAS MODE2 and UNB3M. Three peaks are observed in the value of zenith tropospheric delay for SAAS MODE 1, one in March and the others in February and October with a kind of minimum in August. There is a drop around April to July and later rise around August.

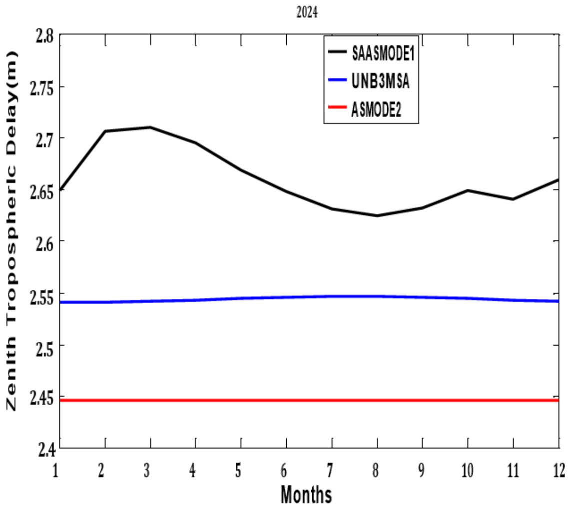

Figure 4: Monthly plot of Zenith tropospheric delay for the year 2024

Figure 5 shows the monthly plot of Zenith tropospheric delay for SAAS MODE1 at Offa for eleven consecutive years. It is observed that there is a seasonal trend in SAAS MODE1 and two peaks are observed generally in the value of zenith tropospheric delay for all the years, one in March and the other one in November with a kind of minimum in August, with the exceptional of the year 2019 and 2020 where three peaks are observed in the values of zenith tropospheric delay for SAAS MODE 1, one in March and the others in February and October with a kind of minimum in august. The year 2017 and 2018 attained their minimum in July. There is a drop at the peak point of every year up to July there about and rises again at their respective minimum point till November with the exceptional years 2020, 2022, 2023, and 2024 which experience their rises till September.

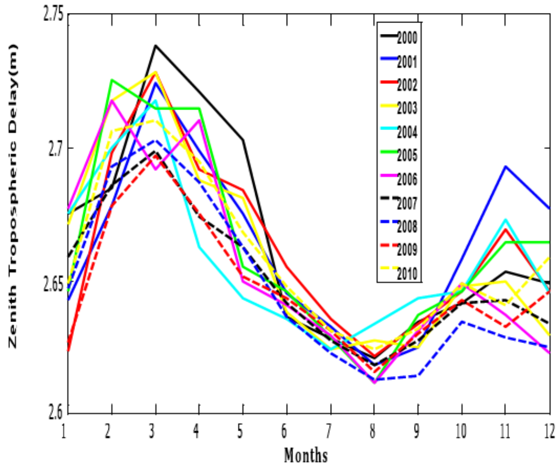

Figure 5: Monthly plot of Zenith tropospheric delay for years 2014 to 2024.

Zenith Delay to Slant Delay

To compare the output of three mapping functions (Chao, Niell, and TANE) at an elevation of 2° to 90°, data for the year 2024 were used. Forth is study, SAAS MODE 1 and SAAS MODE 2 were used.

Figure6showsapanelplotoftropospheric delay as a function of elevation for March 2024. It is observed that the three mapping functions returned almost the same values from elevation 90° to about 20°. Major discrepancies are observed at an elevation of 5° and below in which the TANE value deviated completely from the other two models. This gives Chao and Niella good edge over TANE.As far as the deviations are concerned, the TANE value is higher than the other two

Models by about 30m at the elevation angle of 2°.

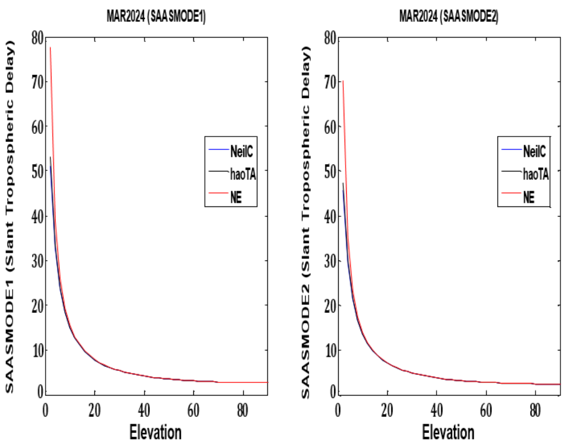

Figure 6: Panel plot of delay as a function of elevation angle for March 2024

International Journal of Advances in Engineering and Management (IJAEM)
Volume 7, Issue 4 April. 2025, pp: 1133-1139 www.ijaem.net ISSN: 2395-5252

Figure 7 shows a panel plot of tropospheric delay as a function of elevation for August 2024. It is observed that the three mapping functions returned almost the same values from elevation 90° to about 20°. Major discrepancies are observed at an elevation of 5° and below in which the TANE value deviated completely from the other two models. This gives Chao and Niella good edge over TANE.As far as the deviations are concerned, the TANE value is higher than the other two models by about 30 m at the elevation angle of 2 °.

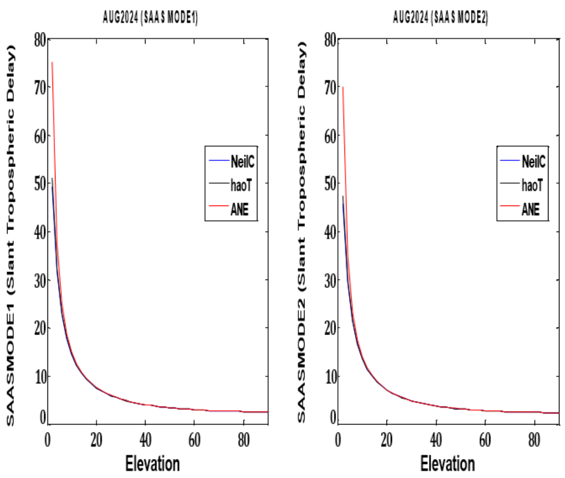

Figure 7: Panel plot of delay as a function of elevation angle for August 2024

Figure 8 shows a panel plot of tropospheric delay as a function of elevation for October 2024. It is observed that the three mapping functions returned almost the same values from elevation 90° to about 20°. Major discrepancies are observed at an elevation of 5° and below in which the TANE value deviated completely from the other two models. This gives Chao and Niella good edge over TANE.As far as the deviations are concerned, the TANE value is higher than the other two models by about 30 m at the elevation angle of 2°.
Based on these observations, we may conclude that the three-mapping function is good as far as the accuracy of the results is concerned. Of course, at a lower elevation angle, one should not use the simple TANE model. However, the mapping functions Chao and Niell are stable at all elevation angles.

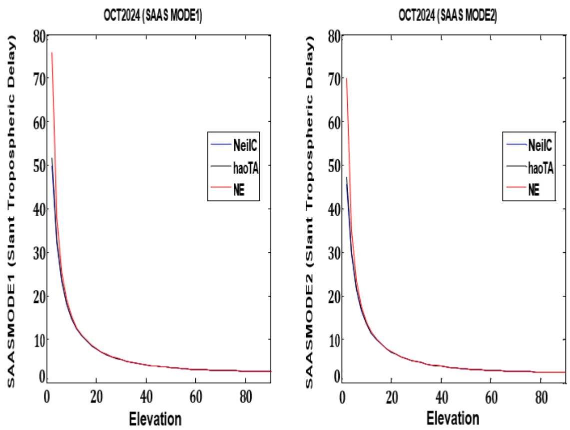

Figure 8: Panel plot of delay as a function of elevation angle for October 2024

Discussion

The Global Positioning System reached operational statusinearly1994andis now operating continuously with the 24-satellite constellation. Traditionally it was used for high-precision geodesy, and the GPS has recently emerged as a powerful tool in atmospheric studies, in particular, climatology and meteorology [9]. Tropospheric delay is one of the sources of error in GPS positioning. The total tropospheric zenith delay can be separated into two components, a delay due to the dry component of the troposphere and the non- dipole component of water vapor refractivity. Slant tropospheric delay is estimated using a mapping function. These delays were computed at monthly intervals for the satellites in view corresponding to the station-satellite direction. The slant tropospheric delays using the Saastamoinen model (driven by tropospheric data) as a reference for computation at the smaller elevation angle of 2^0 to 90^0.
It is observed that in SAAS MODE 1, there is a seasonal trend due to water vapor in the atmosphere. The trend observed in SAAS MODE 1 is similar to the seasonal trend observed in vapor pressure values.
Figure 9 shows the monthly plot of water vapor for the year 2024. Three peaks are observed in the value of zenith tropospheric delay for SAAS MODE 1, one in March and the others in February and October with a kind of minimum in August. There is a drop around April to July and later rise around August. Based on these observations, we may conclude that the SAAS MODE 1 is good as far as the estimation is concerned.

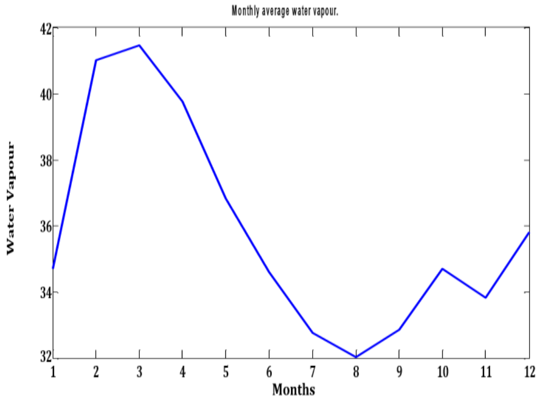

Figure 9: Plot of monthly average water vapor for the year 2024.

IV. CONCLUSION

This study focused on the estimation of tropospheric delay for Offa using three tropospheric delay models, namely the Saastamoinen model (SAAS MODE 1 driven by observed tropospheric data), Saastamoinen model (SAAS MODE 2 driven by the default values) and UNB3M model. The tropospheric data used are for the years 2014 to 2024. The results obtained show that there are seasonal trends in SAAS MODE1 whereas are not observed in SAAS MODE 2 and UNB3M. Two peaks are observed generally in the value of zenith tropospheric delay for SAAS MODE 1 for all the years, one in March and the other one in November with a kind of minimum in August. In the exceptional especially years 2019 and 2020 where three peaks are observed in the values of zenith tropospheric delay for SAAS MODE 1, one in March and the others in February and October with a kind of minimum in August. There is a drop from the peak point March to July there about and later rise around August. To compare the output of three mapping functions (Chao, Niell, and TANE) at an elevation of 2^0 to 90^0, data for the year 2024 were used. For this study, SAAS MODE1 and SAAS MODE2 were used. It is observed that the three mapping functions returned almost the same values from elevation 90° to about 20°. Major discrepancies are observed at an elevation of 5°and below in which the TANE value deviated completely from the other two models. This gives Chao and Niella good edge over TANE.As far as the deviations are concerned, the TANE value is higher than the other two models by about 30 m at the elevation angle of 2°.

Seasonal trends in monthly variations in temperature, pressure, and relative humidity can lead to errors in tropospheric delays. The location of Offa in the equatorial and tropical region (Offa is located on latitude 8.9^0N, and Longitude 4.43^0E, of the equator) makes it susceptible to high tropospheric effect thereby having an adversative effect on the GPS signals, which consequently affects positioning.

REFERENCES

[1]. Skone, S., Atmospheric effects on the satellite navigation system, ENGO 633 Course Lecture Notes, 2023, University of Calgary, Calgary, Canada.

[2]. Bevis, M., S. Businger, S. Chiswell, T. A. Herring, R.A. Anthes, C. Rocken and R. Ware (2016), GPS meteorology: mapping zenith wet delays onto precipitable water, Journal of Applied Meteorology, Vol. 33, pp. 379-386.

[3]. Dodson, A.H., P.J. Shardlow, L.C.M. Hubbard, G. Elgered and P.O.J. Jarlemark (2018), Wet tropospheric effects on precise relative GPS height determination, Journal of Geodesy, No. 70, No. 4, pp. 188-202.

[4]. Bevis, M., S. Businger, T.A. Herring, C. Rocken, R.A. Anthes and R.H. Ware (2014), GPS meteorology: sensing of atmospheric water vapor using the Global Positioning System, Journal of Geophysical Research, Vol. 97, No. D14, pp. 15787-15801.

[5]. Herring, T.A. (2014), Modeling atmospheric delays in the analysis of space geodetic data, Proceedings of Symposium on Refraction of Trans atmospheric Signal in Geodesy, The Netherlands, No. 36, New series, pp. 157-164.

[6]. Ifadis, I.M. (2008), The atmospheric delay of radio waves: modelling the elevation dependence on a global scale, School of Electrical and Computer Engineering, Chalmers University of Technology, Goteborg, Sweden, Technical Report No. 38L, pp. 115.

[7]. Neill, A.E. (2018), Global mapping functions for the atmospheric delay at radio wavelengths, Journal of Geophysical Research, Vol. 111, No. B2, pp. 3227-3246.

[8]. Bar-Sever, Y.E. (2018), Strategies for near real- time estimation of precipitable water vapor, IGS 2018 Analysis Center Workshop Proceedings, pp.165-175.

[9]. Baby, H.B., P. Gole and J. Lavergnat (2010), A model for the tropospheric excess path length of radio waves from surface meteorological measurements, Radio Science, November- December, Vol. 23, No. 6, pp. 1023-1038.

[10]. Bar-Sever, Y.E., and P.M. Kroger (2020), Estimating horizontal gradients of tropospheric path delay with a single GPS receiver, Journal of Geophysical Research, Vol. 103, No. B3, pp. 5019-5035.

[11]. Davis, J.L., G. Elgered, A.E. Neill and C.E. Kuehn (2015), Ground-based measurement of gradients in the wet radio refractivity of air, Radio Science, Vol. 28, No. 6, pp. 10031018.

[12]. Davis, J.L. (2023), Atmospheric water vapor signals in GPS data: Synergies, correlations, signals, and errors, Physics and Chemistry of Earth (A), Vol. 26.

[13]. International GPS Service (IGS) (2023), International GPS service annual report, 2023, IGS Central Bureau, Jet Propulsion Laboratory, Pasadena, Calif., pp. 14-16.

[14]. Kaniuth, K. (2008), A local model for estimating the tropospheric path delay at microwave frequencies, Proceedings of the Fourth International Geodetic Symposium on Satellite Positioning, Austin, Texas, April 28-May 2, Vol. 1, pp. 589-601.

[15]. Mendes, V.B. (2021), Modelling the neutral- atmosphere propagation delay in radiometric space techniques, Ph.D. dissertation, University of New Brunswick, Fredericton, Canada.

[16]. Neill, A.E. (2022), Improved atmospheric mapping functions for VLBI and GPS, Earth Planets Space, No. 52, pp. 699-702.